Effects of Interfacial and Viscous Properties of Liquids on Drop Spread Dynamics

V. Ravi, M. A. Jog[*], and R. M. Manglik
Thermal-Fluids and Thermal Processing Laboratory
University of Cincinnati
Cincinnati, OH 45221-0072 USA

Abstract

An experimental study of the post-impact spreading of liquid droplets on dry horizontal substrates is presented in this paper. The drop spreading and recoil behaviors are captured using a high-speed digital video camera at 2000 frames per second. To ascertain the effects of liquid interfacial and viscous properties, experiments were conducted with five liquids (water, ethylene glycol, propylene glycol, glycerin, and acetic anhydride). A range of drop Weber number from 20 to 120 was considered by altering the height from which the drop is released. Effects of liquid properties on droplet spread-recoil dynamics were determined by comparing the results of liquids with different surface tension but similar viscosity and vice versa. The high-speed photographs of impact, spreading and recoil are shown and the temporal variations of dimensionless drop spread and height are provided in the paper. Results show that changes in liquid viscosity and surface tension significantly affect the spreading and recoil behavior. For a fixed Weber number, lower surface tension promotes greater spreading and higher viscosity dampens recoil. Also, spread, recoil and shape oscillations were more pronounced on a hydrophobic substrate (Teflon) compared to those on a hydrophilic substrate (glass). A detailed comparison of maximum spreads observed in the experiments with those obtained using spread correlations available in the literature show significant differences. Limitations of the available correlations are discussed in the paper.

---

[*]Corresponding author

Introduction

Liquid droplet impact and spreading on dry solid surfaces is an important process in many practical applications. They include industrial spray cooling of hot metal surfaces and spray coating as well as other day to day applications such as inkjet printing. As such the phenomena of droplet impact and spreading on solid surfaces have been addressed by many researchers using experimental, analytical, and computational methods [1-12]. In these studies, the droplet surface evolution has been presented in terms of the spread factor (the ratio of instantaneous spread to initial droplet diameter) and the flattening factor (the ratio of liquid thickness to droplet diameter prior to impact).

The prediction of the maximum spread is useful in design and optimization of coating or cooling processes in many industrial applications. For instance, the cooling of hot metal surfaces is more efficient when the spreading ratio and the rate at which the droplet recedes and spreads on the hot surface are very high. To determine the extent of spreading for a given liquid-substrate combination, the principle of energy conservation has been applied between the instant before impact to the time of maximum spread. From this energy balance, correlations for the maximum spread for pure liquid droplets in terms of the drop Weber number, Reynolds number, and Ohnsorge number have been derived [1-7]. It is recognized that in addition to liquid properties (ρ, σ, μ) and drop velocity, surface energy (hydrophobic or hydrophilic nature of the substrate), interfacial tension, the dynamic contact angle variation, play important role in governing the drop spread/recoil dynamics. Furthermore, the liquid-solid contact angle is affected by the hydrodynamics in the vicinity of the moving contact line which in turn affects the drop spreading and shape evolution [13]. These complex phenomena pose significant challenge in the development of a universal correlation for spread and recoil behavior.

In the present study, we have captured the droplet impact-spreading-recoil phenomena for droplets of five liquids (water, ethylene glycol, propylene glycol, glycerin, and acetic anhydride). The post-impact spreading and recoil behaviors are recorded using a high-speed digital video camera at 2000 frames per second. A range of drop Weber number from 20 to 120 was considered by altering the height from which the drop is released. To ascertain the effects of liquid properties, the results of liquids with different surface tension but similar viscosity and vice versa were compared. A detailed comparison of maximum spreads observed in the experiments with those obtained using spread correlations available in the literature show significant differences. Limitations of the available correlations are discussed in the paper.

Experimental Setup

The experimental setup is shown in Figure 1. A droplet was generated through a flat-tipped stainless steel needle having orifice diameter of 1.19mm. The droplet was allowed to grow until it detached from the tip and fell on the substrate due to gravity. The cleaning process of the substrates is very critical as the surface wetting behavior is sensitive to impurities and roughness of the surface. The substrates are first rinsed with distilled water and subsequently by ethanol and acetone and wiped clean with a low-lint wipe. The clean, dry substrate is placed on the leveling table and is checked for flatness and zero orientation. The phenomenon of droplet impact is captured with a High speed camera system: Hi-DCam II version 3.0 (NAC Image Technology). The camera has an 8× zoom lens which helps capture clear images during the process. A focusing single bulb light system (ARRI) with glossy reflectors and an adjustable stand was used. The light was reflected from a white background to obtain a good picture quality. The camera was aligned in line with the substrate at zero degrees to record the images. The frame rate of the camera was set to 2000fps and the corresponding shutter speed to 1/2000. The resolution of the camera was set to 520 × 1024 which provided a record time of 8.652 seconds.
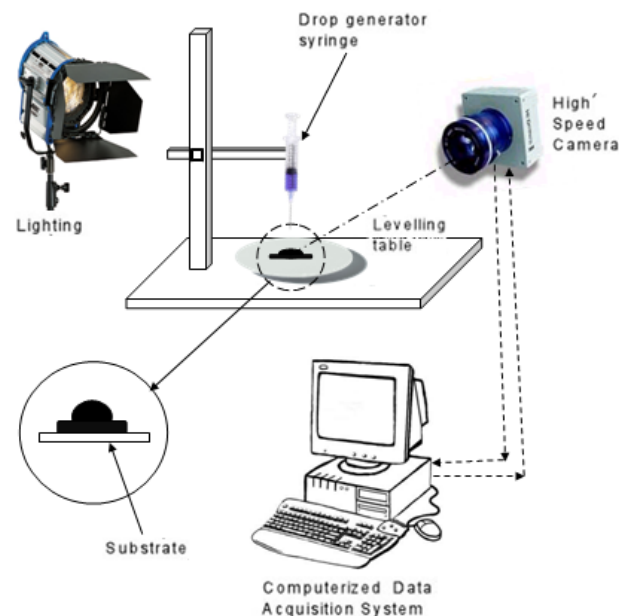

Figure 1. Schematic of experimental data acquisition and analysis set up

Table 1. Physical and interfacial properties of test liquids.

Properties	Water	Acetic Anhydride	Ethylene Glycol	Propylene Glycol	Glycerin
Viscosity (mPa.s)	1	0.806	16	52	749
Surface Tension (dyne/cm)	72.7	31.98	48	36	65.16
Density (kg/m^3)	1000	1077	1115.3	1033	1257
Equilibrium Contact angle on glass (degrees)	23.7	18.3	22.7	20.5	48.3
Equilibrium Contact Angle on Teflon (degrees)	121	74	97	90	120

The captured images were analyzed with the help of an image-processing software (Image-Pro Plus 4.0 by Media cybernetics). There was no noticeable temperature rise in the substrates when they are exposed to this light source during the experimentation process.

Two substrates were used in the experiments. They were Teflon (hydrophobic) and glass (hydrophilic). The test liquids used were distilled water, glycerol, propylene glycol, ethylene glycol and acetic anhydride. The physical and interfacial properties of these liquids are given in Table 1. The liquids were chosen so that the effect of viscosity and surface tension on droplet impact-spreading dynamics could be isolated. For example, propylene glycol and acetic anhydride have nearly the same surface tension at 25 degrees Celsius but their viscosities are very different. Similarly, the viscosity of water and acetic anhydride are almost the same, but their surface tension values are vastly different. Since the diameter of the droplet produced from the needle orifice for each of these liquids is governed by the liquid properties such as surface tension, viscosity and the density, the mean diameter of the droplet is determined using Image-Pro Plus 4.0 from the image just prior to impact. The droplet velocity was determined from a series of photographs taken before impact.

The equilibrium contact angle θ, was determined using the capillary rise technique. The orifice diameter of the glass capillary tube is 0.6mm. The capillary was first rinsed with distilled water and then with acetone and then it was cleaned with the test liquid and was allowed to dry at room temperature. The capillary tube was then immersed vertically into the test liquid. The liquid rises inside the orifice due to capillary action. The rise of the liquid through the capillary orifice was measured. The equilibrium contact angle is calculated using the equation,

$$l = 2\sigma \cos(\theta)/\rho g r \qquad (3)$$

where l is the capillary rise, σ is the surface tension, ρ is the density of the test liquid and r is the radius of the capillary tube orifice. The contact angle thus calculated is the equilibrium contact angle of the test liquid with glass.

The equilibrium contact angle of the test liquids with Teflon was determined by the sessile drop method. A small drop of the liquid was placed on the Teflon substrate and the equilibrium contact angle was measured. The equilibrium contact angle values on both glass and Teflon are also shown in Table 1.

Results and Discussion:

The experiments were performed by varying droplet velocities to cover the range of Weber number from about 20 to 120. The Weber number was restricted to this range to avoid the onset of splashing [14].

Figure 2 shows a sequence of high-speed photographs (impact, maximum spread, maximum recoil, and final equilibrium) that highlight the differences in spread-recoil behavior of different liquids on a hydrophobic (Teflon) substrate at Weber number of about 20. The detailed temporal variations of spread factor and flattening factor are depicted in Figures 3 and 4 respectively. It is seen from Figure 3 that in all cases, the liquid spreads to become a thin layer that recoils under the action of surface tension force. Distilled water has the highest surface tension and low viscosity among the liquids considered here and consequently the water droplet exhibits the strongest recoil. Surface oscillations continue until the viscous dissipation brings the liquid to rest. The effect of fluid viscosity becomes clear when we compare the behavior of water and glycerin droplets. Although surface tension of these two liquids is similar, their viscosities are vastly different (by a factor of 749). The high viscosity of glycerin damps both spread and recoil and glycerin droplet produces a small spread and weak recoil.
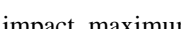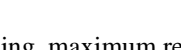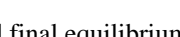
Liquid	Before Impact	Maximum Spread	Maximum Recoil	Equilibrium
Distilled Water				
Acetic Anhydride				
Ethylene Glycol				
Propylene Glycol				
Glycerin				

Figure 2 High-speed photographs of droplet impact, maximum spreading, maximum recoil, and final equilibrium on a hydrophobic surface (Teflon). We ~ 20.
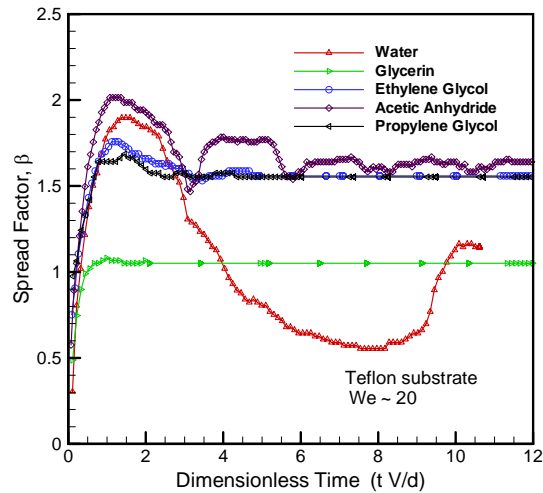
Figure 3. Temporal variation of the spread factor during post-impact spreading on a Teflon substrate. We ~ 20

Figure 4. Temporal variation of the flatness factor during post-impact spreading on a Teflon substrate We ~ 20

A similar pattern is seen in the case of acetic anhydride and propylene glycol, whose surface tension values are comparable but their viscosities differ by a factor of about 65.

The temporal variations of the spread factor and the flattening factor for We ~ 20 on a glass substrate are shown in Figures 5 and 6, respectively. By comparing the spread factor variations on glass (Fig. 5) to those on Teflon (Fig. 3), the effect of substrate wettability can be assessed. The initial spreading stage is dominated by the inertial and viscous forces.

Additionally the substrate wetting behavior plays a role in determining the maximum spread. Acetic anhydride spreads more on glass than on Teflon for all Weber numbers. However, the difference in the maximum spreading ratios of acetic anhydride on glass and Teflon decreases with increasing impact velocity.

During the recoil stage, the substrate wettability is seen to plays a dominant role in governing the drop surface evolution. Distilled water exhibits strong recoil on a Teflon substrate compared to that on a

Figure 5. Temporal variation of the spread factor during post-impact spreading on a glass substrate. We ~ 20

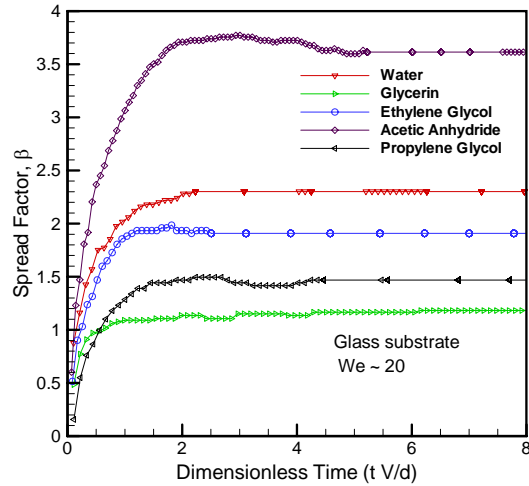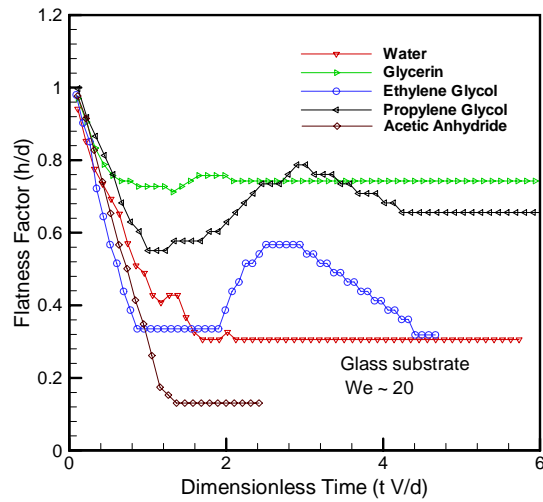
Figure 6. Temporal variation of the flatness factor during post-impact spreading on glass substrate. We ~ 20

glass substrate and undergoes multiple surface oscillations before reaching the equilibrium condition. Acetic anhydride shows a similar difference in recoil behavior on Teflon and glass, although its recoil is weaker compared to water because of lower surface tension. Glycerin and shows very weak recoil and only small shape oscillations due to its high viscosity. Propylene glycol droplet produces damped recoil but it does shows more pronounced shape oscillations compared to glycerin.

Figure 7 shows the variation maximum spread factor on a glass substrate for different Weber numbers for the five liquids considered here. The effect of surface tension and viscosity on the initial spreading process is evident from data presented in
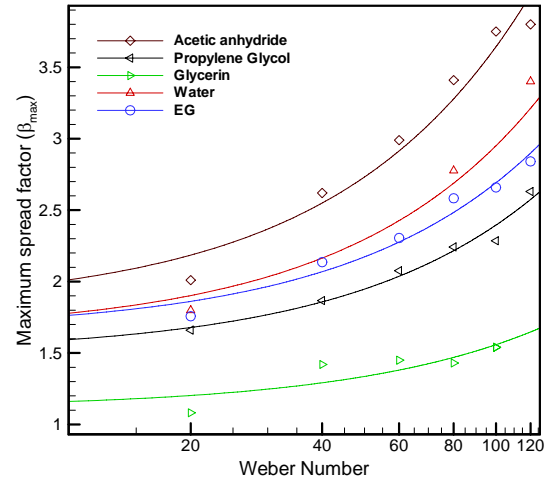

Figure 7. Variation of the maximum spread factor with Weber number for drop impact on a Teflon substrate.

this figure. Low surface tension combined with low viscosity of acetic anhydride facilitates the largest spread factor for all Weber numbers compared to other liquids. Acetic anhydride and propylene glycol have similar values of surface tension but the viscosity of propylene glycol is significantly higher. Not surprisingly, the maximum dimensionless spread for of acetic anhydride is about 40% greater than the maximum spreading ratio of propylene glycol. The important role of viscosity in resisting drop spreading is seen to produce very low maximum spread factors for glycerin and propylene glycol.

Experimental data and correlations:

Prediction of maximum spread of a droplet impacting on a surface is needed in many spray applications so as to design process parameters that lead to desired outcomes. For example, achieving accurate drop spread is important in ink-jet printing, coating of pharmaceutical products, control of solidification in spray deposition, pesticide coating in agricultural sprays, and to control heat transfer in cryogenic spray cooling. Many semi-empirical correlations for prediction of the maximum drop spread are available in literature. These are listed in Table 2. It is known that the process of post-impact spreading is governed by fluid properties (ρ, σ, μ), drop velocity, surface wettability, and the dynamic contact angle variation. The correlations represent attempts to scale these effects and to estimate the maximum spread by applying the principle of energy conservation. One of the earliest correlations is by Jones [1] where he considered liquid viscosity but neglected the effect of liquid-gas interfacial tension altogether. The dependence of the droplet spread on the viscosity of the fluid was investigated by Scheller

and Bousfield [15], using water-glycerin mixture droplet impinging a polysterene substrate. They showed that with increase in viscosity, the dependence of the droplet spread on the impact velocity decreases. Their correlation for the maximum spread ratio included the effects of viscosity, surface tension, and impact velocity in terms of the Reynolds number and the Ohnesorge number based on drop size and velocity prior to impact. Ohnsorge number can be expressed in terms of Reynolds and Weber numbers. To be consistent with other correlations, we have recast Scheller and Bousfield's correlation in terms of Re and We in Table 2. Madejski [2] considered solidification in post-impact spreading and developed a correlation that included viscous dissipation and liquid-gas interfacial tension. However, his model does not include the effect of surface wettability on liquid spreading. Asai et al. [5] proposed a correlation using their data of spreading of ink drops. The applicability of their correlation is limited due to the lack of surface wetting behavior effects. Attempts were made to include such effects using the static contact angle. For example, Mao et al. [7] measured post-impact droplet spread in their experiments with various concentrations of water-sucrose mixture and determined that the maximum spread ratio of the liquid droplets by varying viscosity of the liquid and the impact velocity. They proposed a correlation for the maximum spread ratio as a function of the Weber number, Reynolds number and the static contact angle. Collins et al. [3] and Chandra and Avedisian [4] have used the static contact angle in their semi-empirical correlations as well. More recently, the surface behavior has been considered in terms of the advancing contact angle, for example, Pasandideh-Fard et al. [6] and Ukiwe and Kwok [9]. In most cases, the advancing contact angle information is not readily available and that limits the use of these correlations. When the liquid and the substrate are at different temperatures, the liquid viscosity may change as it spreads and heats (or cools). Yang [16] proposed a correction in terms of viscosity ratio ($\mu_{\text{drop}}/\mu_{\text{wall}}$). Such correction in terms of viscosity ratio is commonly used to incorporate the effects of viscosity variation with temperature on the friction loss and heat transfer in duct flow [17].

We have compared our experimental data for the maximum spread factor with predictions obtained using correlations listed in Table 2 for all liquid-substrate combinations for $20 < We < 120$. As representative cases, data for acetic anhydride is presented for different Weber number in Table 3 and 4 for Teflon and glass substrates, respectively. The comparison shows that the available correlations fail to accurately predict the experimental values.

Table 2. A list of correlations to predict the maximum spread factor $\beta_{\max}$

Authors	Correlation
Jones (1971)	$\beta_{\max} = \left(\dfrac{4}{3}\text{Re}^{1/4}\right)^{1/2}$
Yang (1975)	$\dfrac{We}{2} + 6 = \dfrac{3}{2}\beta_{\max}{}^2 \times \big[1 + \dfrac{3We}{\text{Re}} \times$ $\left(\beta_{\max}{}^2 \ln\beta_{\max} - \left(\beta_{\max}{}^2 - 1\right)/2\right)$ $\times \left(\mu_{drop}/\mu_{wall}\right)^{0.14}\big]$
Madejski (1976)	$\dfrac{3\beta_{\max}{}^2}{We} + \dfrac{1}{\text{Re}}\left(\dfrac{\beta_{\max}}{1.2941}\right)^5 = 1$
Collings et al. (1990)	$\beta_{\max} < \left(\dfrac{We}{3\left(1-\cos\theta\right)}\right)^{1/2}$
Chandra Avedisian (1991)	$\dfrac{3We}{2\,\text{Re}}\beta_{\max}{}^4 + (1-\cos\theta)\beta_{\max}{}^2$ $-\left(\dfrac{1}{3}We + 4\right) \approx 0$
Asai et al. (1993)	$\beta_{\max} = 1 + 0.48We^{0.5} \times$ $\exp\left[-1.48We^{0.22}\,\text{Re}^{-0.21}\right]$
Scheller Bousfield (1995)	$\beta_{\max} = 0.91\left(\text{Re}\sqrt{We}\right)^{0.133}$
Pasandideh-Fard et al. (1996)	$\beta_{\max} = \left[\dfrac{We + 12}{3\left(1-\cos\theta_{adv}\right) + \dfrac{4We}{\sqrt{\text{Re}}}}\right]^{\frac{1}{2}}$
Mao et al. (1997)	$\left[\dfrac{1}{4}\left(1-\cos\theta\right) + 0.2\dfrac{We^{0.83}}{\text{Re}^{0.33}}\right]\beta_{\max}{}^3$ $-\left(\dfrac{We}{12} + 1\right)\beta_{\max} + \dfrac{2}{3} = 0$
Ukiwe & Kwok (2005)	$\left(We + 12\right)\beta_{\max} = 8 + \beta_{\max}{}^3 \times$ $\left[3\left(1-\cos\theta_{adv}\right) + 4\dfrac{We}{\sqrt{\text{Re}}}\right]$

Moreover, there is no unanimity in the predictions obtained using different correlations. Majority of the correlations do not capture the change in maximum spread due to the difference in surface wettability.

Table 3. Comparison of experimental values of maximum spread factor during post-impact spreading of acetic anhydride droplet on Teflon substrate at different Weber numbers with values obtained from various correlations.

Diameter	We	Re	Present study	Jones	Collins	Madejski	Chandra and Avedisian	Mao	Asai	Yang	Scheller and Bousfield
2.18	22.8	1.62 E3	2.01	2.91	3.03	2.72	3.45	2.50	2.23	3.08	2.99
2.23	42.2	2.23 E3	2.62	3.03	4.12	3.60	3.94	2.82	2.60	3.59	3.25
2.16	59.0	2.60 E3	2.99	3.09	4.87	4.14	4.22	3.01	2.84	3.89	3.40
2.11	79.7	2.99 E3	3.41	3.14	5.66	4.62	4.48	3.19	3.08	4.16	3.53
2.06	94.9	3.22 E3	3.75	3.17	6.18	4.90	4.62	3.30	3.23	4.32	3.61
2.15	117	3.65 E3	3.80	3.22	6.86	5.24	4.83	3.46	3.44	4.54	3.72

Table 4. Comparison of experimental values of maximum spread factor during post-impact spreading of acetic anhydride droplet on glass substrate at different Weber numbers with values obtained from various correlations.

Diameter	We	Re	Present study	Jones	Collins et al.	Madejski	Chandra and Avedisian	Mao	Asai	Yang	Scheller and Bousfield
2.19	22.9	1.63E3	3.77	2.91	3.03	2.73	4.72	3.87	2.23	3.08	3.00
2.18	41.2	2.18E3	4.01	3.02	4.07	3.57	4.91	4.06	2.58	3.56	3.24
2.15	58.6	2.59 E3	4.24	3.08	4.86	4.13	5.06	4.24	2.83	3.88	3.39
2.13	80.3	3.01 E3	4.53	3.14	5.68	4.64	5.21	4.43	3.09	4.17	3.53
2.05	94.8	3.21 E3	4.62	3.17	6.18	4.90	5.27	4.61	3.23	4.32	3.61
2.19	119	3.72 E3	4.87	3.23	6.93	5.27	5.45	4.79	3.47	4.57	3.73

The correlation give by Chandra and Avedisian [4] gives different values for Teflon and glass substrates but it significantly over-predicts the maximum spread in both cases. Other correlations that use advancing contact angle have not been compared because the advancing contact angle information was not available on glass and Teflon surfaces. It is clear that difficulties in scaling the complex interactions of liquid properties, surface wettability, dynamic contact angle variation, and liquid velocity have hindered the development of a universal correlation.

Conclusions:

The post-impact spreading and recoil of liquid droplets on a hydrophobic (Teflon) and a hydrophilic (glass) substrate is experimentally investigated. The drop spreading and recoil behaviors are captured using a high-speed digital video camera at 2000 frames per second. The experiments were conducted with five liquids (water, ethylene glycol, propylene glycol, glycerin, and acetic anhydride). A range of drop We-

ber number from 20 to 120 was considered by altering the height from which the drop is released.

The spread and recoil behavior is presented in terms of the temporal variations of the spread factor (instantaneous spread/initial drop diameter) and flattening factor (instantaneous liquid thickness/drop diameter). Liquid properties play an important role in determining the post-impact spread-recoil behavior. As such for a fixed Weber number, the spread-recoil behavior is significantly different for each liquid. It is seen that lower surface tension promotes greater spreading and produces weaker recoil. However, higher viscosity damps both spreading as well as recoil. Surface wettability significantly affects the droplet-surface interaction. For a fixed Weber number, stronger recoil was observed on Teflon (hydrophobic) compared to that on glass (hydrophilic) for all liquids. Comparison of experimental data for the maximum spread factor with predictions obtained using different correlations available in literature shows that not only the correlations fail to accurately

predict the maximum spread but also there is no unanimity in their predictions.

Nomenclature

d drop diameter
g   gravitational acceleration
h instantaneous spread
l capillary rise
r radius of the capillary tube
Re   Reynolds Number $\left(\rho V d / \mu \right)$
V drop velocity at impact
We   Weber Number $\left(\rho V^2 d / \sigma \right)$
β spread factor ($= h/d$)
β_{max} maximum spread factor
ρ Density of the fluid
σ Surface Tension of the fluid
θ Contact angle
μ Viscosity of the fluid
μ_{drop} Viscosity of the droplet at room temperature
μ_{wall} Viscoity of the droplet at wall temperature

References

1. Jones, H., *Journal of Physics: D Applied Physics*, 4: 1657-1660 (1971)
2. Madejski, J., *International Journal of Heat and Mass Transfer*, 19: 1009-1013 (1976)
3. Collings, E.W., Markworth, A. J., McCoy, J. K., and Saunders, J.H., *Journal of Material Science*, 25: 3677-3682 (1990)
4. Chandra, S., and Avedisian, C. T., *Proceedings of Royal Society A: Mathematical and Physical Sciences*, 432: 13-41 (1991)
5. Asai, A., Shioya, M., Hirasawa, S., and Okazaki, T., *Journal of Imaging Science and Technology*, 37: 205-207 (1993)
6. Pasandideh-Fard, M., Qiao, Y. M., Chandra, S., and Mostaghimi, J., *Physics of Fluids*, 8: 650-658 (1996)
7. Mao, T., Kuhn, D.C.S., and Tran, H., *AIChE Journal*, 43: 2169-2179 (1997)
8. Rioboo, R., Marengo, M., and Tropea, C., *Atomization and Sprays*, 11: 155-165 (2001)
9. Ukiwe, C., and Kwok, K. Y., *Langmuir*, 21: 666-673 (2005)
10. Sikalo, S., and Ganic, E.N., *Experimental Thermal Fluid Science*, 31: 97-110 (2006)
11. Yarin, A.L., *Annual Review of Fluid Mechanics*, 38: 159-192 (2006)
12. Gatne, K.P., Jog, M. A., and Manglik, R. M., *Langmuir*, 25: 8122-8130 (2009)
13. Sikalo, S., Wilhelm, H. D., Roisman, I. V., Jakirlic, S., and Tropea, C., *Physics of Fluids*, 17: 062103-1-12 (2005)
14. Mundo, C., Sommerfeld, M., and Tropea, C., *International Journal of Multiphase Flow*, 21: 151-173 (1995)
15. Scheller, B.L., and Bousfield, D. W., *AIChE Journal*, 41: 1357-1367 (1995)
16. Yang, W.-J.," Theory of vaporization and combustion of liquid drops of pure substances and binary mixtures on heated surfaces", Report number 535, pp. 423-455, University of Tokyo, 1975
17. Harms, T., Jog, M. A., and Manglik, R. M, *Journal of Heat Transfer*, 120: 600-605 (1998)